# Temperature dependent deformation mechanisms in pure amorphous silicon

M. S. R. N. Kiran, B. Haberl, J. S. Williams, and J. E. Bradby

Citation: Journal of Applied Physics **115**, 113511 (2014); doi: 10.1063/1.4869136
View online: http://dx.doi.org/10.1063/1.4869136
View Table of Contents: http://scitation.aip.org/content/aip/journal/jap/115/11?ver=pdfcov
Published by the AIP Publishing

# Temperature dependent deformation mechanisms in pure amorphous silicon

M. S. R. N. Kiran,[a] B. Haberl, J. S. Williams, and J. E. Bradby
*Department of Electronic Materials Engineering, Research School of Physics and Engineering, Australian National University, Canberra, Australian Capital Territory 0200, Australia*

(Received 6 February 2014; accepted 8 March 2014; published online 21 March 2014)

High temperature nanoindentation has been performed on pure ion-implanted amorphous silicon (unrelaxed *a*-Si) and structurally relaxed *a*-Si to investigate the temperature dependence of mechanical deformation, including pressure-induced phase transformations. Along with the indentation load-depth curves, *ex situ* measurements such as Raman micro-spectroscopy and cross-sectional transmission electron microscopy analysis on the residual indents reveal the mode of deformation under the indenter. While unrelaxed *a*-Si deforms entirely via plastic flow up to 200 °C, a clear transition in the mode of deformation is observed in relaxed *a*-Si with increasing temperature. Up to 100 °C, pressure-induced phase transformation and the observation of either crystalline (r8/bc8) end phases or pressure-induced *a*-Si occurs in relaxed *a*-Si. However, with further increase of temperature, plastic flow rather than phase transformation is the dominant mode of deformation. It is believed that the elevated temperature and pressure together induce bond softening and "defect" formation in structurally relaxed *a*-Si, leading to the inhibition of phase transformation due to pressure-releasing plastic flow under the indenter. © *2014 AIP Publishing LLC*.
[http://dx.doi.org/10.1063/1.4869136]

## INTRODUCTION

Diamond cubic silicon (*dc*-Si) undergoes a series of phase transformations with increasing pressure.[1,2] At a pressure of ~11 GPa *dc*-Si transforms to a metallic phase with the *β*-Sn structure [(*β*-Sn)-Si], which is accompanied by a 22% increase in density and undergoes further transformations to metastable phases r8 and bc8 on pressure release (below ~10 GPa), as observed by high-pressure diamond anvil,[3–7] theoretical studies,[8] and indentation experiments.[9–11] Formation of metallic phase during loading was observed using *in situ* electrical resistance measurement[12,13] and scanning spreading resistance microscopy.[14] Recently, Gerbig *et al.*[15] confirmed the earlier theoretical predictions using a state-of-art *in-situ* Raman microspectroscopy experimentation, including the direct observation of the formation of the (*β*-Sn)-Si phase during indentation and the subsequent transformations to the r8 and bc8 metastable phases, and their transformation pressures, during unloading. To the best of the author's knowledge this is the only *in-situ* indentation study presently available. However, often pressure-induced (PI) amorphous Si (rather than crystalline r8/bc8 phases) has been observed as the final structure in case of indentation experiments.[16]A recent detailed study that provides the most comprehensive model of the conditions that are required for the formation of crystalline and amorphous phases during indentation loading and unloading, maximum indentation load, tip geometry and including the role of unloading strain rate for the appearance of newly formed phases in crystalline Si is the work of Gerbig *et al.*[17] For example, "fast" unloading (from ms to about 1 s) tends to result in PI *a*-Si, while "slow" unloading (typically > several seconds) results in a mixture of the crystalline r8 and bc8 Si phases as sufficient time is available for the nucleation of these new structures. Data obtained from indentation load-displacement (P-h) curves can be used to identify these structural changes that occur in the indented volume during unloading. In particular, an "elbow" or "pop-out" event will appear in the unloading curve,[16,18–20] as signatures of either an amorphous structure or crystalline phase formation, respectively. Importantly, however, the presence of any such distinctive feature (pop-out or elbow) in the unloading curve is a reliable indicator that metallic (*β*-Sn)-Si formed on loading, i.e., that a pressure-induced phase transition had occurred. Gerbig *et al.*[21] performed a statistical indentation study and detailed analysis on the pop-in, pop-out and elbow events during indentation of Si, including assessments of pressures during loading and unloading at which events occur, and the effects of crystal orientation on the phase transformation behavior. The above literature provides a complete and detailed understanding of the indentation induced phase transformations in crystalline Si at room temperature.

Although *dc*-Si is well studied, mechanical studies of the pure amorphous forms are scarce. While mean bond lengths and bond angles are similar for both *dc*-Si and pure, voidless *a*-Si (both are tetrahedrally coordinated and the density of *a*-Si is only 1.8% lower than *dc*-Si),[22] they can exhibit distinctly different physical properties such as mechanical and electrical properties due to lack of long range ordering.[23] The structural and dynamical properties of *a*-Si have been extensively investigated theoretically using classical force fields,[24] tight binding approximations[25] and *ab initio* simulations[26] but the deformation mechanism[27–29] in pure *a*-Si upon application of pressure remains unclear. This is because *a*-Si is different from amorphous metallic glasses due to the highly directional covalent bonding that can make deformation processes more complex. Moreover, understanding the

[a]Author to whom correspondence should be addressed. Electronic mail: kiran.mangalampalli@anu.edu.au

 

pressure-induced deformation in *a*-Si is of technological interest due to its wide use in photovoltaic cells,[30] and micro-electromechanical systems [MEMS].[31,32] In general, *a*-Si prepared by vapor deposition methods usually contains voids, and thus can easily absorb impurities such as hydrogen, oxygen, and carbon upon exposure to air.[33] In addition, reduced Si-Si network strain was observed in *a*-Si layers that contained hydrogen since atomic hydrogen is known as a successful passivator of dangling bonds.[34] However, ion-implantation has been recognized as a successful technique to produce pure and voidless amorphous layers.[35,36] Thus, pure ion-implanted *a*-Si is an ideal amorphous material for studying pressure-induced deformation mechanisms. The current study uses *a*-Si prepared by self ion-implantation as described in the experimental section.

The properties of amorphous silicon vary significantly depending on the thermal history and preparation conditions.[36] For example, when ion-implanted *a*-Si is annealed (at 450 °C, for 30 min in $N_2$ atmosphere) it undergoes "structural relaxation" or short-range ordering.[35,36] Annealing reduces the number of "imperfections" in the network, resulting in a decrease in the average bond-angle distortion.[35,36] Relaxed *a*-Si is considered to be close to a fully coordinated continuous random network (CRN). However, just as every single crystal is non-ideal and has some defects, so too do real amorphous materials. Thus, relaxed *a*-Si will also contain imperfections or defects in terms of dangling bonds, vacancy and interstitial-like defects. Less perfect amorphous materials such as unrelaxed *a*-Si will have a much higher defect density. Interestingly it has been shown that these two states of *a*-Si, unrelaxed and relaxed, exhibit a very different behavior under indentation testing.[37,38] At room temperature, a pop-out is observed in the unloading curve, and both Raman micro-spectroscopy and cross-section transmission electron microscopy (XTEM) studies of the residual indent impressions revealed that the relaxed state undergoes a phase transformation under loading above ~11 GPa. Indeed, r8 and bc8 phases are obtained under appropriate unloading conditions[37] (similar to *dc*-Si), but no evidence of phase transformation was found in the unrelaxed *a*-Si indented under identical conditions.[38]

Although the stress fields under the indenter favor phase transformations at room temperature in Si, temperature is another important parameter that has been little studied to date. One study observed new features related to kinks on the unloading curve when relaxed *a*-Si was indented at 125 °C. It was suggested that the smaller kink-like pop-outs may be the final transformation of remaining volumes of ($\beta$-Sn)-Si to r8/bc8 during the unloading cycle.[39] In contrast, Bhuyan *et al.*[40] have observed a pop-out in the *P-h* curve when relaxed *a*-Si was indented at 175 °C, but no further evidence of phase transformation was given. Until now, there has been no detailed study of phase transformation in various forms of *a*-Si as a function of temperature in order to understand how temperature influences the mode of deformation.

In this current work, we indent two forms of *a*-Si under Berkovich indentation at various temperatures between 25 °C and 200 °C to gain insight into the competing deformation mechanisms of plastic flow and phase transformation. This study employs *in situ* high temperature indentation and the *ex situ* characterization techniques of Raman micro-spectroscopy and XTEM.

## EXPERIMENTAL

Si ion-implantation into a Czochralski-grown Si (100) wafer *p*-doped with boron to a resistivity of 10–20 Ω-cm was undertaken to produce continuous *a*-Si films of ~2 $\mu$m thickness. Implantation was performed at liquid nitrogen temperature using the ANU 1.7 MV NEC tandem high-energy ion implanter with wafer surfaces tilted 7° to the beam direction to minimize ion channeling. A fluence of $1 \times 10^{15}$ ions/cm$^2$ was used for each of the multiple energies of 0.08, 0.5, 1.0, 1.5, and 2.0 MeV. Samples were probed for their composition and film thickness using Rutherford backscattering spectrometry under channeling conditions, and for microstructure by cross-sectional transmission electron microscopy. Results confirmed that pure *a*-Si films of ~2 $\mu$m thickness, continuous to the surface, were obtained. The as-implanted material is referred to as "unrelaxed *a*-Si." Selected samples were furnace annealed at 450 °C for 30 min in a nitrogen atmosphere and such samples are called "relaxed *a*-Si." This annealing process is known to "relax" but not re-crystallize the amorphous layers.[37]

Raman micro-spectroscopy is very sensitive to the short range (≤1 nm) order (SRO) of an amorphous network. A typical Raman spectrum from both unrelaxed *a*-Si and relaxed *a*-Si is shown in Fig. 1. This figure shows four broad peaks in the spectrum, the TA (transverse acoustic), the LA (longitudinal acoustic), the LO (longitudinal optic), and the TO (transverse optic) peaks.[41,42] The characteristic broad TO-peak can be correlated with the degree of SRO and whether the state of *a*-Si is relaxed or unrelaxed.[41,42] In particular, the peak width ($\Gamma$) can be correlated to the average bond-angle distortion ($\Delta\theta$) within a continuous random network, with a lower peak width correlating to a lower $\Delta\theta$. It can be seen that the half-width ($\Gamma/2$) of the TO-like peak decreases as a result of thermal treatments. $\Gamma/2$ can be

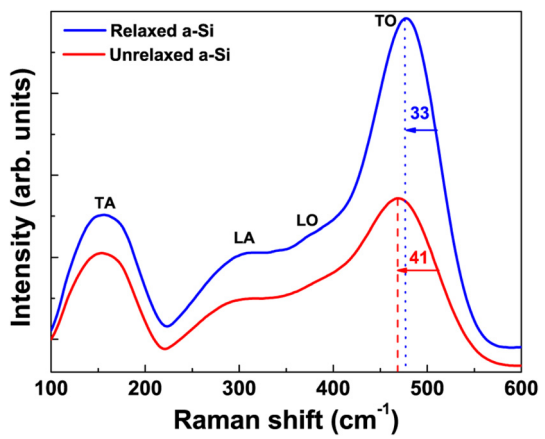


FIG. 1. Two typical Raman spectra of amorphous silicon. Raman spectra of relaxed *a*-Si (top) and unrelaxed *a*-Si (bottom). The upper curve shows the half width of the TO peak $(\Gamma/2) = 33\,\text{cm}^{-1}$ and the lower curve $\Gamma/2 = 41\,\text{cm}^{-1}$.

converted to $\Delta\theta$ using the empirical relationship derived by Beeman[42]

$$\Gamma/2\ (\mathrm{cm}^{-1}) = 7.5 + 3\,\Delta\theta\ (\mathrm{degree}). \quad (1)$$

For pure *a*-Si, $\Gamma/2$ is found to decrease by ~20% after annealing (at 450 °C for 30 min), consistent with previous literature.[41]

Nanoindentation was performed on both unrelaxed and relaxed forms of *a*-Si, using a Hysitron TriboIndenter (Minneapolis, USA). A three sided pyramidal diamond Berkovich tip with an end radius of ~100 nm was used in this study. The indentations were performed at 25, 50, 100, 150, and 200 °C on a heating stage.[43,44] A peak load of 10 mN was reached in 10 s (loading segment) and unloading was performed at two different rates (i.e., 10 or 0.2 $\mathrm{mNs}^{-1}$) with a hold period of 5 s at the peak load. To gain adequate statistics on pop-out events and the formation of r8/bc8 phases, 25 indents were performed at each temperature for both slow unloading (0.2 mN/s) and fast unloading (10 mN/s). In order to minimize the effects of thermal drift, the sample and stage were held at the testing temperature for 60 min before performing the first indent and 60 min hold between every two indents. The array of indentations was performed in the "piezoautomation mode" of the TriboIndenter, which allows the tip to always be in contact with the surface (at a very low load of typically 2 $\mu$N) even while moving from one indent location to another. The total time required to perform the 25 indents was approximately 26 h. The distance between indents was set as 10 $\mu$m to avoid the effect of previous strain fields on the fresh indent. Temperature accuracy has been measured with the aid of two thermocouples, one placed under the heating plate (the control thermocouple) and the other one on the sample. A temperature variation of 18–22 °C was consistently observed between heating plate and the sample. Therefore, the temperature was always set 20 °C higher to achieve the required temperature of the sample.

The structure of the end phases was determined using a Renishaw 2000 Raman micro-spectroscopy instrument with a 632.8 nm laser (with an incident power of 2.10 mW) focused to a spot of diameter ~2 $\mu$m from the middle of the residual indent impression (indents are ~1 $\mu$m in diameter). Since the diameter of the laser spot and size of the indent impression are similar, the Raman spectra contain information from both background *a*-Si and transformed material (if any) within the indent impression.

A Philips CM 300 instrument operating at an accelerating voltage of 300 kV was used for the conventional bright-field transmission electron microscopy (TEM) imaging of samples prepared using focussed ion beam milling and the "pluck-out" method.[45] Prior to loading the samples into the focused ion beam (FIB) system, a thin ~10 nm layer of gold was sputtered onto the surface to avoid charging effects. A platinum layer was deposited on top of the gold-coated surface using the FIB system (first with the electron beam (~100 nm) and then with the ion-beam ~1 $\mu$m) to shield the samples from damage during the ion milling process. In the TEM, selected area diffraction patterns (SADP) were taken using a ~300 nm aperture directly beneath the residual indent impression to determine the structures of the end phases.

Before presenting the results of this study the following points are worth noting. As the maximum temperature studied is 200 °C, we can neglect any increased formation of oxide on the surface since Si is known to only react significantly with oxygen beyond 400 °C.[46] Also, since the *a*-Si is produced with self ion-implantation in the current study, the samples are pure and void free.[35,36]

## RESULTS AND DISCUSSION

Figure 2 shows *P*-*h* curves obtained from unrelaxed *a*-Si loaded to 10 mN at various temperatures starting from 25 °C to 200 °C and at slow and fast unloading rates. Both loading and unloading portions are smooth without any discontinuities suggesting homogeneous deformation. The quantitative data obtained from the above curves are given in Table I. It is evident that the maximum penetration depth, $h_{max}$, at 10 mN increases with increasing temperature, from ~246 ± 1 nm at 25 °C to ~254 ± 2 nm at 200 °C (~4% increase) suggesting enhanced plastic flow at elevated temperatures. Similarly, the final depth ($h_f$) also increases with increasing temperature, again consistent with increases plastic flow. The elastic recovery data also presented in this table is discussed below.

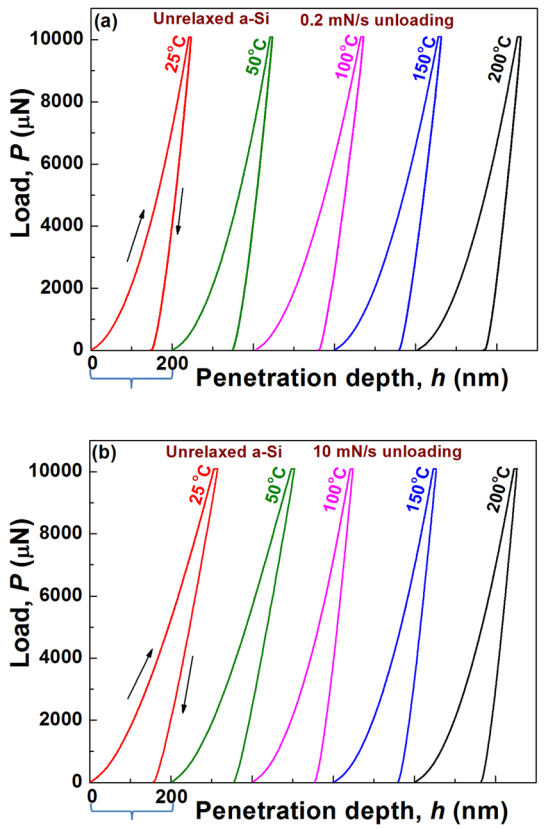


FIG. 2. Load-displacement curves obtained from indentation of unrelaxed *a*-Si at various temperatures and at (a) 0.2 mN/s and (b) 10 mN/s unloading rates. Loading rate (1 mN/s) and hold period (5 s) are the same for all experiments. Displacements shifted to greater depths for clarity.

TABLE I. Quantification of *P-h* curves obtained from nanoindentation of unrelaxed *a*-Si at various temperatures. The error bar presented here is estimated from the average of 25 indents.

| | Max. depth, $h_{max}$ (nm) | Final depth, $h_f$ (nm) | | Elastic recovery (%) | |
|---|---|---|---|---|---|
| Temp., $T$ °C | At 1 mN/s loading | 0.2 mN/s unload | 10 mN/s unload | 0.2 mN/s unload | 10 mN/s unload |
| 25 | 246 ± 1 | 145 ± 2 | 154 ± 2 | 41 ± 0.6 | 37 ± 1.1 |
| 50 | 248 ± 1 | 146 ± 3 | 155 ± 2 | 41 ± 0.5 | 36 ± 0.6 |
| 100 | 248 ± 2 | 146 ± 2 | 155 ± 3 | 41 ± 0.6 | 36 ± 0.6 |
| 150 | 252 ± 2 | 156 ± 1 | 158 ± 2 | 38 ± 0.9 | 36 ± 0.6 |
| 200 | 254 ± 2 | 160 ± 1 | 166 ± 3 | 36 ± 0.3 | 34 ± 0.9 |

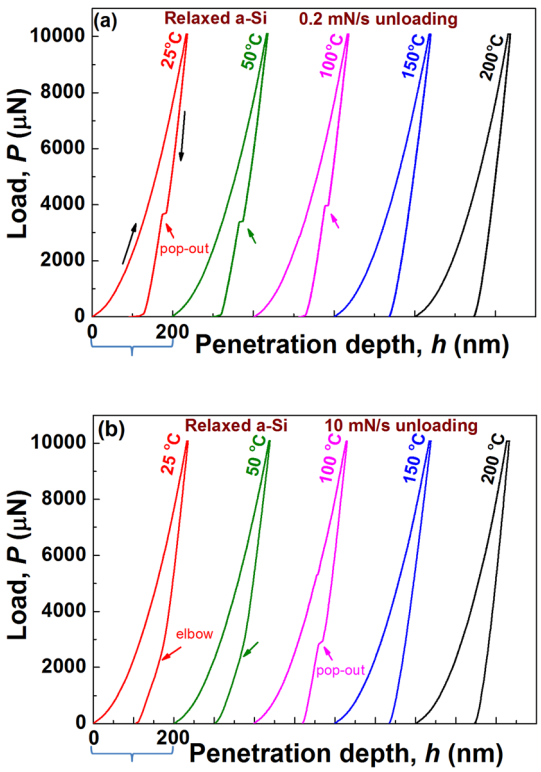


FIG. 3. Load-displacement curves obtained from indentation on relaxed *a*-Si at various temperatures and at (a) 0.2 mN/s and (b) 10 mN/s unloading rates. Loading rate (1 mN/s) and hold period (5 s) are same for all experiments. Displacements shifted to greater depths for clarity.

In contrast, the indentation response from the relaxed *a*-Si under similar experimental conditions shown in Fig. 3 is very different. The information from the *P-h* curves is quantified and presented in Table II. It can be seen that $h_{max}$ varies insignificantly with increasing temperature from 25 °C to 200 °C. However, distinctly different $h_f$ values upon complete unloading were seen at different temperatures and at different unloading rates. This suggests different modes of elastic recovery or phase transformation on unloading. While the average $h_f$ is 128 ± 2 nm when pop-outs are present in the unloading curve [Fig. 3(a)], it is 107 ± 2 nm following elbow behavior [Fig. 3(b)], and 140 ± 3 nm for smooth featureless unloading curves (at elevated temperatures of 150 °C and 200 °C). In addition, a depth of 117 ± 1 nm was observed exclusively for the fast unloading case at 100 °C [Fig. 3(b)] wherein the unloading curves exhibit kink-like pop-out with the smallest pop-out width ($h_{pop\text{-}out} \sim 4$ nm).

Although, the loading part of the *P-h* curves is smooth [Fig. 3(a)], a clear discontinuity ("pop-out") is observed on slow unloading up to 100 °C in the case of relaxed *a*-Si. During a fast unload, it is interesting to note that the pop-out event is seen only at 100 °C but an elbow is seen at both 25 °C and 50 °C, as shown in Fig. 3(b). An elbow is known to be indicative of the formation of PI *a*-Si under the indenter.[13] Despite this intriguing result, which will be discussed in more depth below, it is clear that in both the fast and slow unloading cases phase transformation (as suggested by pop-out or kink-like discontinuities in the unloading curve) would appear to be occurring up to 100 °C. At 150 °C and 200 °C, however, the *P-h* curves do not exhibit any such discontinuities, but are similar to the curves observed in the unrelaxed *a*-Si case, suggesting plastic flow is now the dominant deformation mechanism.

For unrelaxed *a*-Si, the elastic recovery (estimated using indentation energies)[47] at room temperature was close to 40% but reduced to ~35% at 200 °C, consistent with enhanced plastic deformation at elevated temperatures.

TABLE II. Quantification of *P-h* curves obtained from nanoindentation on relaxed *a*-Si at various temperatures. The error bar presented here is estimated from the standard deviation of 25 indents. Note that the elastic recovery cannot meaningfully be obtained from unloading curves when a phase transformation has occurred.

| | Max. depth, $h_{max}$ (nm) | Final depth, $h_f$ (nm) | | Elastic recovery (%) | |
|---|---|---|---|---|---|
| Temp., $T$ °C | At 1 mN/s loading | 0.2 mN/s unload | 10 mN/s unload | 0.2 mN/s unload | 10 mN/s unload |
| 25 | 237 ± 1 | 128 ± 2 | 107 ± 1 | … | … |
| 50 | 237 ± 1 | 128 ± 2 | 102 ± 2 | … | … |
| 100 | 239 ± 2 | 129 ± 1 | 117 ± 1 | … | … |
| 150 | 241 ± 2 | 136 ± 2 | 137 ± 2 | 43 ± 0.8 | 43 ± 0.5 |
| 200 | 240 ± 2 | 145 ± 2 | 147 ± 1 | 39 ± 1.2 | 38 ± 0.9 |

Interestingly, relaxed *a*-Si also exhibits similar recovery (see Table II) beyond 100 °C suggesting the plastic deformation mechanism at elevated temperatures is similar for both forms of *a*-Si. It is only meaningful to obtain the elastic recovery and plastic energy under conditions of "pure" plastic flow since, when phase transformations occur, there are large (and often sudden) density changes and consequential changes in tip "penetration" under constant load indentation.[21] Consequently, when the load/unload curves are not smooth (i.e., pop-out and elbow events occur on unloading) for the relaxed *a*-Si case, no entries are made for elastic recovery in Table II. Nevertheless, it is possible to obtain information on these parameters for unrelaxed and relaxed *a*-Si above 100 °C. In such cases, the area bounded by the loading and unloading curves represents the plastic energy absorbed.

It is interesting to further consider the consequences of phase transformation and pure plastic deformation by analyzing the shape of the unloading curves and magnitudes of the maximum and final penetration depths for both forms of *a*-Si. The relevant data is shown in Fig. 4. The difference in the $h_{max}$ at the same peak force (10 mN) between the different forms of *a*-Si is due to the lower hardness (and different deformation mechanism at temperatures at or below 100 °C as we show later) for unrelaxed *a*-Si (~9.8 GPa) compared to relaxed *a*-Si (~10.7 GPa).[48] The $h_{max}$ and $h_f$ for unrelaxed *a*-Si at 10 mN load and at 25 °C are ~246 ± 1 nm and 150 ± 2 nm, respectively, irrespective of the unloading rates

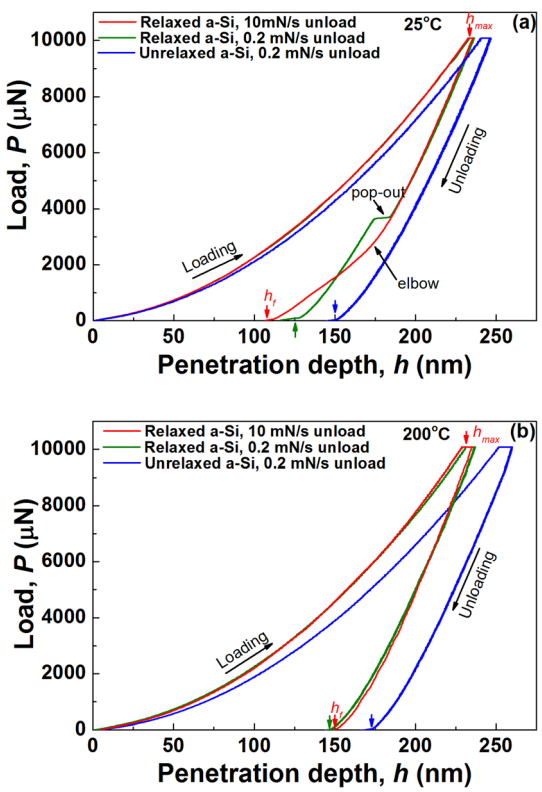


FIG. 4. Comparison of *P-h* curves for both the unrelaxed and relaxed *a*-Si obtained at 25 °C and 200 °C to show the differences in unloading curves, which are signature responses of the mode of deformation or phase transformation under the indenter. The maximum penetration depth at 10 mN and the final penetration depths were represented with $h_{max}$ and $h_f$, respectively. The increased creep at 200 °C is due to enhanced plastic behavior of the material at elevated temperature.

used. At 200 °C, a 4% increase in the $h_{max}$ and 8% decrease in the elastic recovery for the unrelaxed *a*-Si case are attributed to enhanced plasticity due to material flow under the indenter. However, for relaxed *a*-Si, $h_{max}$ is 239 ± 2 nm and varies insignificantly with increasing temperature. This suggests a similar resistance is offered by the material against the indenter penetration, despite different deformation mechanisms (at ≤100 °C and >100 °C). This in turn suggests that although "defects" within the amorphous network (in terms of broken bonds, vacancy and interstitials-like defects) may be formed under the indenter with the application of pressure, their density is not as high as in the case of unrelaxed *a*-Si, where they allow the indenter to penetrate freely into the network. The 4% increase in the $h_{max}$ with increasing temperature in the case of unrelaxed *a*-Si with its large dangling bond density supports the above argument.[22] Furthermore, a significant variation can be noted for $h_f$ with changing unloading rate. When there is a pop-out (0.2 mN/s unloading case), the $h_f$ was recorded as 127 ± 3 nm, while it is 107 ± 2 nm for the elbow case. While the higher $h_f$ in the case of pop-out is due to the formation of the r8/bc8 phases, which are ~10% (Ref. 49) less dense than (*β*-Sn)-Si, lower $h_f$ is attributed to gradual formation of an amorphous volume, which is >20% less dense than the (*β*-Sn)-Si phase.[50] The kink-like pop-out at 100 °C during fast unloading with the $h_f$ of 117 ± 1 nm may be suggestive of the presence of both crystalline phases and an amorphous volume, thus the final depth is close to an average of $h_{f\ (pop\text{-}out)}$ and $h_{f\ (elbow)}$. Therefore, it can be concluded that the relaxed *a*-Si up to 100 °C has undergone phase transformation. However, at 200 °C, the *P-h* curves from both the amorphous forms are very smooth without such pop-out and elbow behavior, as evident from Fig. 4(b). More surprisingly, both the $h_f$ and $h_{max}$ values for the relaxed *a*-Si at 200 °C, irrespective of unloading rate are very similar to the values for unrelaxed *a*-Si at 25 °C (See-Tables I and II). This suggests that the mode of deformation in relaxed *a*-Si under the indenter at elevated temperatures is also via "defect" induced plastic flow, similar to the unrelaxed *a*-Si case. It is also evident from Fig. 4 that the creep increases with increasing temperature for both relaxed and unrelaxed *a*-Si, confirming temperature-enhanced, time-dependent plastic deformation in both the cases. However, since the unrelaxed state is expected to have a larger number of defects incorporated into the network, higher creep is observed.

Now let us confirm our argument on the presence or absence of phase transformation based on indentation results (shape of load/unload curves) by *ex-situ* characterization. Figure 5 shows representative Raman spectra obtained from indented unrelaxed *a*-Si at both slow and fast unloading rates. Except for the a broad amorphous TO peak at 480 $cm^{-1}$, no extra peaks corresponding to crystalline Si phases were found, indicating the material underwent homogeneous plastic deformation at all temperatures irrespective of unloading rate. This fits extremely well with the absence of pop-out/elbow events during unloading in the *P-h* curves (Fig. 2). The continuous increase in peak intensity with increasing temperature can be attributed to the early stages of structural relaxation in unrelaxed *a*-Si, although no fully

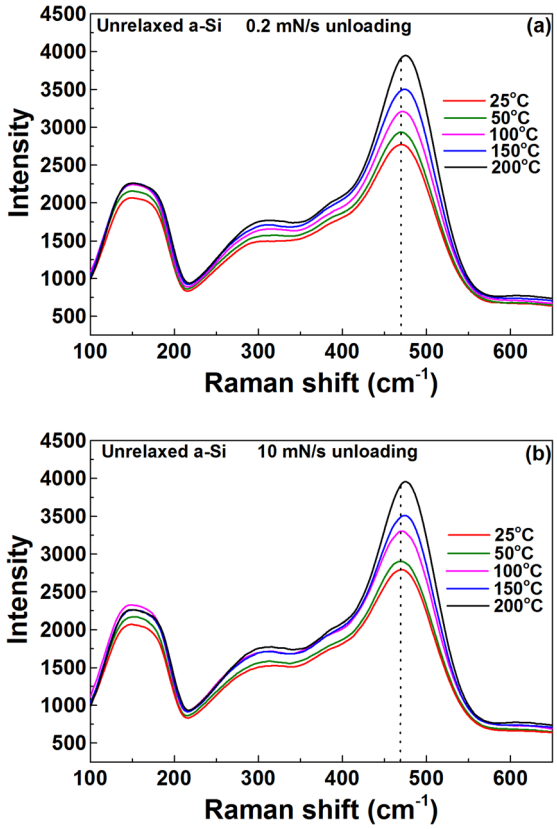


FIG. 5. Raman spectra obtained from indents in unrelaxed *a*-Si at various temperatures and at (a) slow unloading and (b) fast unloading. It is clear from the graphs that an increase in peak intensity and decrease in full width at half maximum (FWHM) with increasing temperature indicates partial structural relaxation with increasing temperature. No extra peaks that correspond to the r8 and bc8 phases are observed, signifying that the dominant deformation mode is via plastic flow.

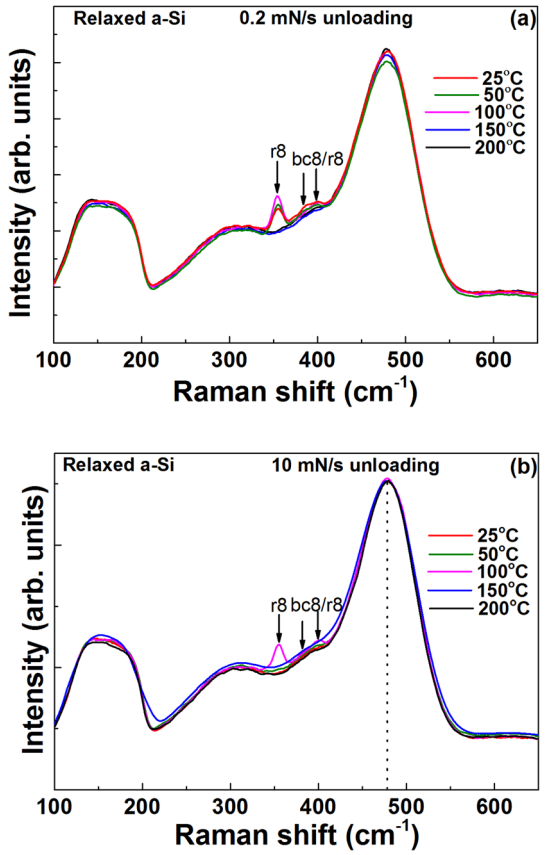


FIG. 6. Raman spectra obtained from indents in relaxed *a*-Si at various temperatures and at (a) slow unloading, (b) fast unloading. The extra peaks at the lower frequency side of the TO peak belong to r8/bc8 phases that are observed consistently only up to 100 °C during slow unloading. In contrast, such Raman peaks are observed only at 100 °C during fast unloading. In both the cases at elevated temperatures, no signatures of crystalline Si phases are observed; signifying that the dominant deformation mode is via plastic flow.

relaxed state is reached during elevated temperature indentation.[41]

Figure 6 shows Raman spectra obtained from indented relaxed *a*-Si at both slow and fast unloading rates. In the case of relaxed *a*-Si we note that, as expected, the width of the TO peak does not change with temperature. This observation confirms a fully relaxed *a*-Si state. In contrast to unrelaxed *a*-Si, some Raman spectra show a clear presence of r8/bc8 peaks from indents made up to 100 °C during slow unloading. These are absent at higher temperatures (i.e., >100 °C). However, during fast unloading, r8/bc8 peaks were observed from the indent made only at 100 °C, as shown in Fig. 6. The absence of crystalline Si Raman peaks at 25 °C and 50 °C supports the observation of elbows in the *P*-*h* curves and transformation of ($\beta$-Sn)-Si to the PI *a*-Si end phase.

Figure 7 shows the probability of phase transformation (determined from pop-outs, elbows, and Raman results) against indentation temperature for both relaxed and unrelaxed *a*-Si. The probability of formation of either crystalline and/or amorphous end phases is essentially 100% at all temperatures up to 100 °C, as shown in Fig. 7. Pop-outs (when observed) occurred in approximately the same position for all temperatures during both unloading rates. Interestingly, the pop-out magnitude decreases from 11 ± 1 nm to 8 ± 1 nm with increasing temperature up to 100 °C. The unstable nature of the ($\beta$-Sn)-Si structure during pressure release and the complex nucleation kinetics for r8/bc8 formation means that it is not possible to correlate this trend with the transformed volume. Yet, a decrease in the pop-out magnitude with increasing temperature is a notable observation and may

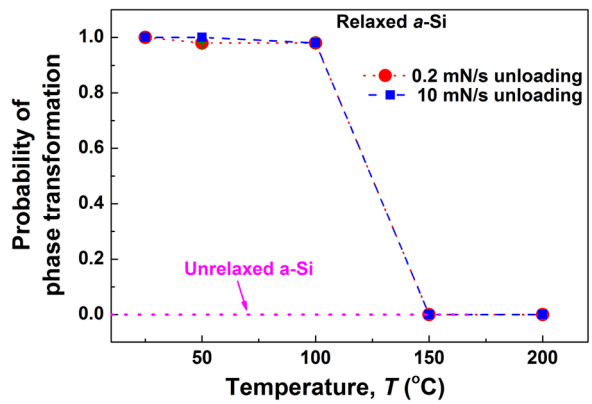


FIG. 7. Probability of high pressure phases detected by both Raman microspectroscopy and indentation unloading features is plotted as a function of temperature for both the fast and slow unloading rates for relaxed *a*-Si samples. Up to 100 °C, the probability for phase transformation is essentially 100% but a sudden transition is observed thereafter representing a change in the mode of deformation. The dotted line at the bottom for unrelaxed *a*-Si shows that the probability of phase transformation is zero at all temperatures studied.

suggest that some r8/bc8 nucleation occurs prior to pop-out at 100 °C.[51]

Figure 8 shows XTEM bright-field images of residual indents made in relaxed *a*-Si at various temperatures during slow unloading, along with SADP of the region immediately beneath the residual indents. Indents at 25 °C and 100 °C show the clear presence of crystalline Si phases within the deformed volume. However, at 150 °C and 200 °C only *a*-Si is observed, thus confirming the conclusions from the indentation and Raman microscopy results. Indeed, the SADPs captured for 150 °C and 200 °C show only diffuse rings (characteristic of *a*-Si) without any additional spots. At 25 °C and 100 °C, the SADP consists of electron diffraction spots corresponding to r8/bc8, along with low intensity amorphous rings. These extra diffraction spots (indicated with circles) are consistent with results from previous work[38] as arising from r8/bc8. It is interesting to note that the disappearance of crystalline Si phases at 150 °C indicates a very sharp transition in the mode of deformation, i.e., from phase transformation to plastic flow. Moreover, the pile-up height also increases with temperatures beyond 100 °C for relaxed *a*-Si. Although Fig. 8 does not show this presence of pile-up formation very clearly, scanning probe microscopy (SPM) images taken using the Hysitron and their cross-sectional profiles across the residual indents have revealed (not shown here) such pile-up behavior. This confirms enhanced plastic flow beyond 100 °C for relaxed *a*-Si, behavior that can also be attributed to the different deformation modes. While the pile-up below 100 °C is due to flow of the soft metallic ($\beta$-Sn)-Si phase, it is due to plastic flow of the *a*-Si matrix beyond 100 °C.

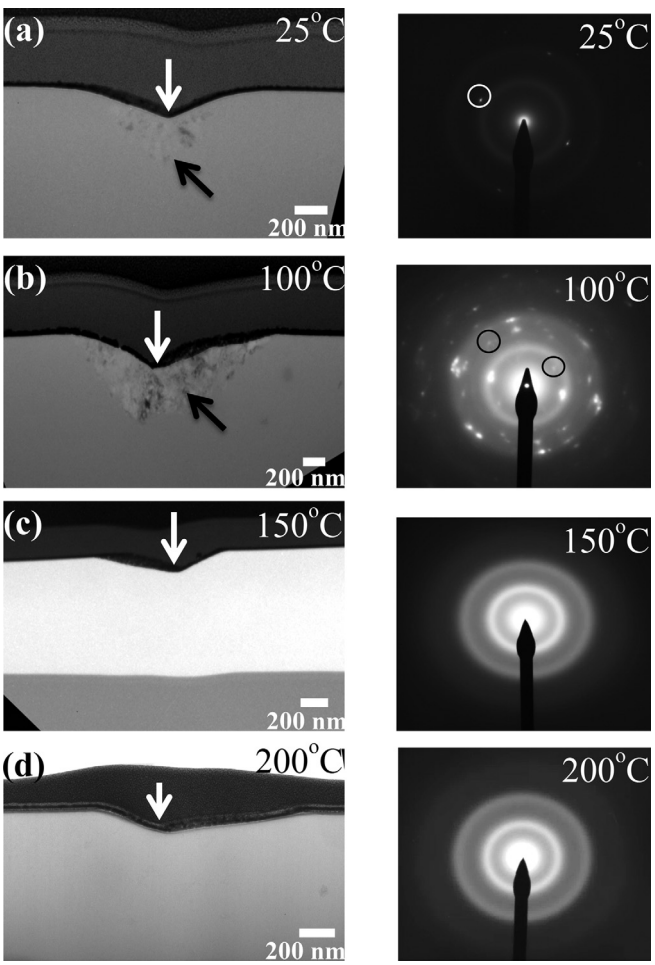


FIG. 8. Bright-field XTEM images of relaxed *a*-Si indented at various temperatures at a load of 10 mN with an unloading rate of 0.2 mN/s. (a) 25 °C, (b) 100 °C, (c) 150 °C, and (d) 200 °C. White arrows indicate the indentation direction. Corresponding selected area diffraction patterns from under the residual indent impressions were used to identify the crystal structure of newly formed phases. Diffraction spots from r8/bc8 are indicated with circles in the SADPs. A ~ 10 nm gold layer and platinum protection layers are clearly visible in all the images.

Before discussing the detailed deformation mechanisms in both unrelaxed *a*-Si and relaxed *a*-Si, it is imperative to consider their fundamental structural differences. When *dc*-Si is amorphized using high energy self-ion implantation, its density reduces by ~2%.[35] Relaxation by thermal annealing was not found to further influence the density of the *a*-Si structure.[52,53] Relaxed *a*-Si has a coordination number of less than 4, typically about 3.8 (Ref. 34) and is voidless.[34] It is widely believed that the structural topology of relaxed *a*-Si can best be represented by a CRN model;[38] however, this topic is still under debate.[54,55] Nonetheless, it is clear that, while unrelaxed *a*-Si is a very defective state of *a*-Si, defect annihilation during thermal annealing will result in a CRN-like network with strong tetrahedral bonding.[56] Therefore, the deformation mechanisms under indentation of the two forms of *a*-Si can reasonably be expected to be different, as in fact is the case at room temperature.[38,48]

Now let us discuss the temperature dependent deformation mechanisms of both forms of *a*-Si. The current study confirms that the deformation mechanism in unrelaxed *a*-Si, irrespective of loading and unloading rates, is via plastic flow and this process is largely temperature independent. Recently, Aji *et al.*[41] investigated the probability for unrelaxed *a*-Si to phase transform under indentation testing after the *a*-Si had been annealed for 30 min at different temperatures. This study found that *a*-Si starts to phase transform under indentation following annealing of the *a*-Si at temperatures $\geq$340 °C (for 30 min). This fits well with our observation of the absence of phase transformations in unrelaxed *a*-Si during indentation up to 200 °C. Moreover, our study shows that the degree of plasticity increases with increasing temperature as evidenced by changes in $h_{max}$ and $h_f$ of the residual indent after complete unloading. The presence of a high defect or dangling bond density[57,58] in unrelaxed *a*-Si would appear to allow the material to flow plastically by propagation of defects and dangling bonds upon application of pressure.[59,60] Increasing temperature to 200 °C enhances plastic flow, suggesting that defect propagation is enhanced. Such plastic flow can be envisaged as a collective (homogeneous) movement of dangling bonds and other defects somewhat akin to kink-mediated dislocation movement observed in metals. Therefore, our study clearly shows that a temperature up to 200 °C does not affect this deformation behavior in unrelaxed *a*-Si.

In contrast, it is possible to induce phase transformations in relaxed *a*-Si at room temperature by indentation pressure of $\geq$10 GPa as explained above.[37,61] During indentation, relaxed *a*-Si films transform to the metallic ($\beta$-Sn)-Si phase during loading similar to *dc*-Si, with further transformation to the crystalline r8/bc8 phases during unloading.[37] The fact

that we cannot observe phase transformation in relaxed *a*-Si beyond 100 °C is somewhat surprising, given that previous study of *dc*-Si provided some evidence for phase transformation up to 200 °C (Ref. 40) and also that the end phases (r8/bc8) are stable up to 200 °C,[62] as outlined below. We therefore have to consider the following question: Does relaxed *a*-Si undergo a phase transformation on loading to metallic (*β*-Sn)-Si or its high-density amorphous form at elevated temperatures, but then transforms back to *a*-Si on unloading?

This scenario is extremely unlikely for the following reasons. First if 22% more dense (*β*-Sn)-Si was formed on loading, a transformation back to *a*-Si would lead to a large reduction in density and a consequential large drop in penetration depth ($h_{max}$-$h_f$) on unloading, as shown in Fig. 4(a), even if the transformations occurred continuously to give smooth unloading curves. Indeed in comparison with the 25 °C and 100 °C relaxed *a*-Si cases in Fig. 4(a), where a pop-out or elbow gives rise to a large difference between $h_{max}$ and $h_f$, the 150 °C and 200 °C unloading curves indicate a substantially smaller $h_{max}$-$h_f$ value that is consistent with the values for the plastically deforming unrelaxed *a*-Si case. Second, if r8/bc8 crystalline Si phases formed at 150 °C and 200 °C on unloading, based on previous work[38,62] this volume would transform to a further crystalline Si structure, known tentatively as "Si-XIII" (structure as yet unknown) and ultimately to *dc*-Si as annealing continued. Indeed, Ruffell *et al.*[62] found that the r8/bc8 phases, initially formed in relaxed *a*-Si (from 25 °C indentation), started to anneal out only when annealed at 200 °C for almost an hour. In this case the transformation pathway was thought to be to *dc*-Si *via* hexagonal Si (*hd*-Si) and/or "Si-XIII." While a transformation from r8/bc8-Si to *a*-Si has been previously reported by Ge *et al.*,[63] it should be noted that the annealing was done on electron-transparent (<100 nm-thick) samples and hence the structures formed on heating could vary significantly from that of the bulk behaviour. In the present experiments, indentation was performed in a total time of 65 s (10 s loading, 5 s hold and then either 50 s or 1 s unloading) and the *P*-*h* curves obtained in this short time did not show any evidence of pop-outs or elbows at 150 °C or 200 °C. We therefore do not expect full annealing of crystalline Si phases to *dc*-Si in such a short time period. Hence these arguments strongly suggest that phase transformation is highly unlikely to have occurred at 150 °C and 200 °C in relaxed *a*-Si and the most likely deformation mode is plastic deformation.

Figure 9 shows a schematic of the low and high temperature behavior of relaxed *a*-Si under pressure. At temperatures up to 100 °C, phase transformation is favored in the rigid 4-fold coordinated *a*-Si matrix. At ~10 GPa, the (*β*-Sn)-Si structure forms and further transforms on unloading to r8/bc8 or PI *a*-Si depending on unloading rate. Since the deformation mechanism is temperature dependent, it is somewhat surprising that there is an insignificant change in $h_{max}$ between the phase transformation regime and the plastic deformation regime. Up to 100 °C the pressure generated under the indenter is highly confined and aids the phase transformation. However, a further increase in temperature induces bond softening in the relaxed amorphous network, defect formation (bond breaking) and material flow under pressure. The newly formed defects and their propagation under the indenter in turn favour plastic flow and inhibit the pressure build-up under the indenter. Evidently, the recovery of the compressed material upon removal of pressure is significantly smaller beyond 100 °C, similar to the plastic flow behavior of the unrelaxed *a*-Si case. Furthermore, significant pile-up outside of the indent region is consistent with a plastic volume that extends significantly into the matrix under increasing pressure. While the pile-up formation is small below 100 °C and due to the flow of the ductile (*β*-Sn)-Si

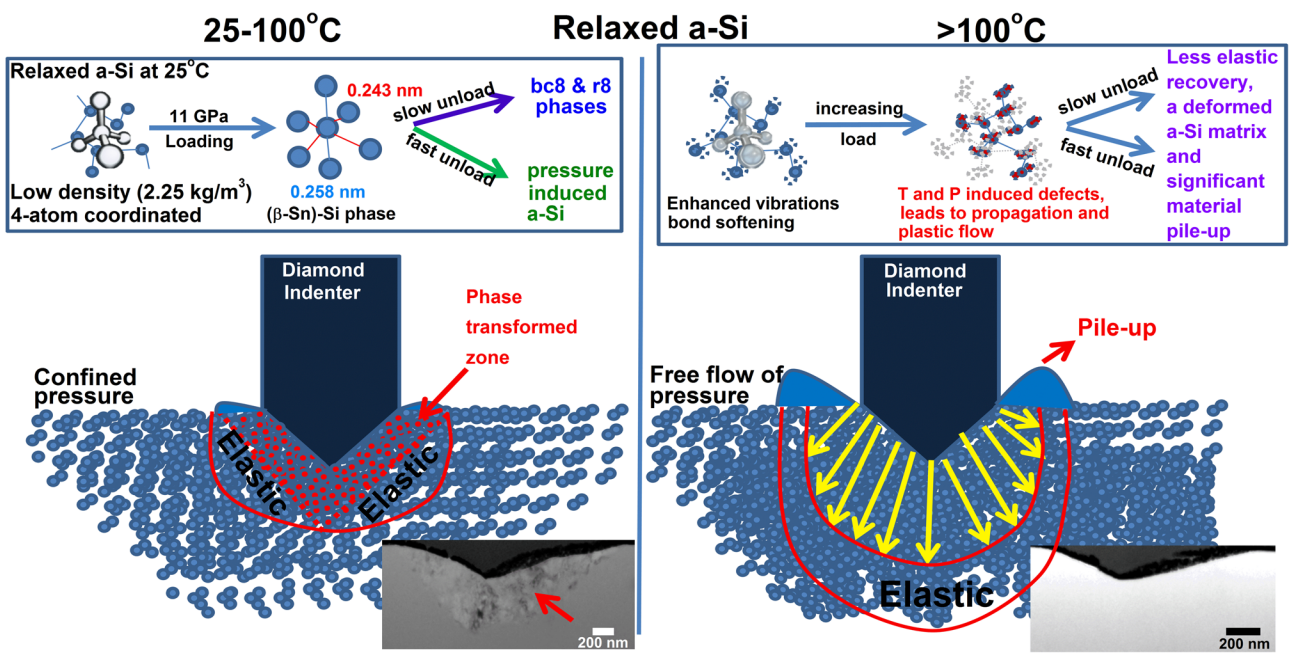


FIG. 9. A schematic diagram based on XTEM observations to explain the deformation of relaxed *a*-Si at various temperatures. It should be noted that pile-up is present at all temperatures after indentation: however, at elevated temperatures its magnitude increased due to enhanced plastic flow.

phase at the contact radius of the indenter, significant pile-up is observed at elevated temperatures (figure not shown here), which is due to an enhanced plastic flow of the amorphous material. The large material propagation and release around the indenter prevents the pressure build-up under the indenter from reaching the transformation pressure. Therefore, we suggest that structural bond softening at temperatures $\geq$150 °C in relaxed *a*-Si favors "defect" formation in the *a*-Si matrix during indentation and propagation under increasing pressure, allowing the material to deform plastically.

## CONCLUSIONS

*In-situ* high temperature indentation has been performed on unrelaxed and relaxed *a*-Si to investigate the temperature dependence of the pressure-induced phase transformation behavior. Our experimental findings reveal that unrelaxed *a*-Si deforms entirely via plastic flow under the indenter at all temperatures. However, up to 100 °C relaxed *a*-Si phase transforms to the metallic ($\beta$-Sn)-Si structure on loading when the pressure reaches ~11 GPa and further transforms to r8/bc8 or PI *a*-Si on unloading, depending on the unloading rate. Beyond this temperature, deformation in relaxed *a*-Si is similar to unrelaxed *a*-Si, i.e., via plastic flow, as confirmed by indentation curves, Raman microspectroscopy, and XTEM. We believe that the elevated temperature and pressure together induce bond softening and defect formation in structurally relaxed *a*-Si. Such defects propagate under pressure and cause substantial plastic flow that prevents the pressure under the indenter from reaching the transformation pressure threshold. We believe that this work is both technologically and scientifically important because understanding the phase transformations and defect-mediated deformation under both temperature and pressure, as well as the stability of new phases, is extremely important for semiconductor processing technologies, particularly if such phases along with *a*-Si are to be used widely in the electronics industry. Moreover, mechanical characterization of *a*-Si at elevated temperature may not only provide further insights in to the dynamics of the pressure and temperature induced phase transformation behaviour of *dc*-Si but may indeed be useful for understanding the deformation mechanisms in other covalently bonded amorphous networks. To the best of the authors' knowledge this is the first report that demonstrates the instability of phase transformations in pure relaxed a-Si under the application of both temperature and pressure. Further studies are in progress to fully understand the phase transformation behavior in the relaxed form of *a*-Si at elevated temperatures using *in-situ* electrical characterization.

## ACKNOWLEDGMENTS

This work has been supported by the Australian Research Council. The Australian National Fabrication Facility (ANFF), ACT Node is acknowledged for use of their FIB facility for the preparation of TEM samples and the Australian Microscopy and Microanalysis Research Facility is access to electron microscopy facilities at ANU. J.E.B. gratefully acknowledges the Australian Research Council for a Future Fellowship.

[1]R. J. Needs and A. Mujica, Phys. Rev. B **51**, 9652 (1995).
[2]D. R. Clarke, M. C. Kroll, P. D. Kirchner, R. F. Cook, and B. J. Hockey, Phys. Rev. Lett. **60**, 2156 (1988).
[3]J. C. Jamieson, Science **139**, 762 (1963).
[4]H. Olijnyk, Phys. Rev. Lett. **68**, 2232 (1992).
[5]J. Z. Hu, L. D. Merkle, C. S. Menoni, and I. L. Spain, Phys. Rev. B **34**, 4679 (1986).
[6]J. Crain, G. J. Ackland, J. R. Maclean, R. O. Piltz, P. D. Hatton, and G. S. Pawley, Phys. Rev. B **50**, 13043 (1994).
[7]R. O. Piltz, J. R. Maclean, S. J. Clark, G. J. Ackland, P. D. Hatton, and J. Crain, Phys. Rev. B **52**, 4072 (1995).
[8]K. J. Chang and M. L. Cohen, Phys. Rev. B **31**, 7819 (1985).
[9]G. M. Pharr, W. C. Oliver, and D. S. Harding, J. Mater. Res. **6**, 1129 (1991).
[10]G. M. Pharr, W. C. Oliver, R. F. Cook, P. D. Kirchner, M. C. Kroll, T. R. Dinger, and D. R. Clarke, J. Mater. Res. **7**, 961 (1992).
[11]E. R. Wepplmann, J. S. Field, and M. V. Swain, J. Mater. Sci. **30**, 2455 (1995).
[12]V. Gridneda, Yu. V. Milman, and V. I. Trefilov, Phys. Status Solidi A **14**, 177 (1972).
[13]J. E. Bradby, J. S. Williams, and M. V. Swain, Phys. Rev. B **67**, 085205(1-9) (2003).
[14]K. Mylvaganam, L. C. Zhang, P. Eyben, J. Mody, and W. Vandervorst, Nanotechnology **20**, 305705 (2009).
[15]Y. B. Gerbig, C. A. Michaels, A. M. Forster, and R. F. Cook, Phys. Rev. B **85**, 104102 (2012).
[16]T. Juliano, V. Domnich, and Y. Gogotsi, J. Mater. Res. **19**, 3099 (2004).
[17]Y. B. Gerbig, S. J. Stranick, and R. F. Cook, Phys. Rev. B **83**, 205209 (2011).
[18]V. Domnich, Y. Gogotsi, and S. Dub, Appl. Phys. Lett. **76**, 2214 (2000).
[19]J. E. Bradby, J. S. Williams, J. Wong-Leung, M. V. Swain, and P. Munroe, Appl. Phys. Lett. **77**, 3749 (2000).
[20]G. M. Pharr, W. C. Oliver, and D. R. Clarke, J. Elec. Mater. **19**, 881 (1990).
[21]Y. B. Gerbig, S. J. Stranick, and R. F. Cook, J. Mater. Res. **24**, 1172 (2009).
[22]J. S. Custer, M. O. Thompson, D. C. Jacobson, J. M. Poate, S. Roorda, W. C. Sinke, and F. Spaepen, Appl. Phys. Lett. **64**, 437 (1994).
[23]D. E. Carlson and C. R. Wronski, *in Amorphous Semiconductors*, edited by M. H. Brodsky (Springer-Verlag, Berlin, 1979), pp. 287–329.
[24]H. Balamane, T. Halicioglu, and W. A. Tiller, Phys. Rev. B **46**, 2250 (1992).
[25]N. Bernstein, J. L. Feldman, and M. Fornari, Phys. Rev. B **74**, 205202 (2006).
[26]I. Stich, R. Car, M. Parrinello, and S. Baroni, Phys. Rev. B **39**, 4997 (1989).
[27]A. Kerrache, N. Mousseau, and L. J. Lewis, Phys. Rev. B **83**, 134122 (2011).
[28]A. S. Argon and M. J. Demkowicz, Metall. Mater. Trans. A **39**, 1762 (2008).
[29]A. Kerrache, N. Mousseau, and L. J. Lewis, Phys. Rev. B **84**, 014110 (2011).
[30]J. I. Pankove and D. E. Carlson, Annu. Rev. Mater. Sci. **10**, 43 (1980).
[31]D. M. Follstaedt, J. A. Knapp, and S. M. Meyers, J. Mater. Res. **19**, 338 (2004).
[32]C. Iliescu and B. Chen, J. Micromech. Microeng. **18**, 015024 (2008).
[33]S. Saitoh, T. Sugii, H. Ishiwara, and S. Furukawa, Jpn. J. Appl. Phys. **20**, L130 (1981).
[34]N. Maley and J. S. Lannin, Phys. Rev. B **36**, 1146 (1987).
[35]D. L. Williamson, S. Roorda, M. Chicoine, R. Tabti, P. A. Stolk, S. Acco, and F. W. Saris, Appl. Phys. Lett. **67**, 226 (1995).
[36]S. Roorda, W. C. Sinke, J. M. Poate, D. C. Jacobson, S. Dierker, B. S. Dennis, D. J. Eaglesham, F. Spaepen, and P. Fuoss, Phys. Rev. B **44**, 3702 (1991).
[37]B. Haberl, J. E. Bradby, S. Ruffell, and J. S. Williams, J. Appl. Phys. **100**, 013520 (2006).
[38]B. Haberl, J. E. Bradby, M. V. Swain, J. S. Williams, and P. Munroe, Appl. Phys. Lett. **85**, 5559 (2004).
[39]S. Ruffell, J. E. Bradby, J. S. Williams, D. M. Paniagua, S. Tadayyon, L. L. Coastworth, and P. R. Norton, Nanotechnology **20**, 135603 (2009).

[40]S. K. Bhuyan, J. E. Bradby, S. Ruffell, B. Haberl, C. Saint, and J. S. Williams, MRS Commun. **2**, 9 (2012).
[41]L. B. B. Aji, S. Ruffell, B. Haberl, J. E. Bradby, and J. S. Williams, J. Mater. Res. **28**, 1056 (2013).
[42]D. Beeman, R. Tsu, and M. F. Thorpe, Phys. Rev. B **32**, 874 (1985).
[43]V. Bhakhri and R. J. Klassen, J. Mater. Sci. **41**, 2259 (2006).
[44]J. C. Trenkle, C. E. Packard, and C. A. Schuh, Rev. Sci. Instrum. **81**, 073901 (2010).
[45]H. Saka, J. Vac. Sci. Technol. B **16**, 2522 (1998).
[46]H. Kakiuchi, H. Ohmi, M. Harada, H. Watanabe, and K. Yasutake, Appl. Phys. Lett. **91**, 161908 (2007).
[47]J. C. Tan, J. D. Furman, and A. K. Cheetham, J. Am. Chem. Soc. **131**, 14252 (2009).
[48]B. Haberl, L. B. B. Aji, J. S. Williams, and J. E. Bradby, J. Mater. Res. **27**, 3066 (2012).
[49]J. S. Williams, Y. Chen, J. Wong-Leung, A. Kerr, and M. Swain, J. Mater. Res. **14**, 2338 (1999).
[50]B. Haberl, A. C. Y. Liu, J. E. Bradby, S. Ruffell, J. S. Williams, and P. Munroe, Phys. Rev. B **79**, 155209 (2009).
[51]S. Ruffell, J. E. Bradby, J. S. Williams, and P. Munroe, J. Appl. Phys. **102**, 063521-8 (2007).
[52]K. Laaziri, S. Kycia, S. Roorda, M. Chicoine, J. L. Robertson, J. Wang, and S. C. Moss, Phys. Rev. B **60**, 13520 (1999).
[53]J. S. Custer, M. O. Thompson, J. M. Poate, S. Roorda, W. C. Sinke, and F. Spaepen, Mater. Res. Soc. Symp. Proc. **157**, 689 (1989).
[54]M. M. J. Treacy and K. B. Borisenko, Science **335**, 950 (2012).
[55]S. Roorda and L. J. Lewis, Science **338**, 1539 (2012).
[56]B. Haberl, S. N. Bogle, T. Li, I. McKerracher, S. Ruffell, P. Munroe, J. S. Williams, J. R. Abelson, and J. E. Bradby, J. Appl. Phys. **110**, 096104 (2011).
[57]S. Roorda, J. S. Custer, W. C. Sinke, J. M. Poate, D. C. Jacobson, A. Polman, and F. Spaepen, Nucl. Instr. and Meth. B **59–60**, 344 (1991).
[58]S. Roorda, J. M. Poate, D. C. Jacobson, B. S. Dennis, S. Dierker, and W. C. Sinke, Appl. Phys. Lett. **56**, 2097 (1990).
[59]M. J. Demkowicz and A. S. Argon, Phys. Rev. B **72**, 245205 (2005).
[60]M. J. Demkowicz and A. S. Argon, Phys. Rev. Lett. **93**, 025505(1–4) (2004).
[61]B. Haberl, M. Guthrie, D. Sprouster, J. S. Williams, and J. E. Bradby, J. Appl. Crystallogr. **46**, 758 (2013).
[62]S. Ruffell, B. Haberl, S. Koenig, J. E. Bradby, and J. S. Williams, J. Appl. Phys. **105**, 093513 (2009).
[63]D. Ge, V. Domnich, and Y. Gogotsi, J. Appl. Phys. **95**, 2725 (2004).